Theor. Appl. Climatol. 89, 37–49 (2007)
DOI 10.1007/s00704-006-0243-7
Printed in The Netherlands

Theoretical and Applied Climatology

[1] National Meteorological Services Agency, Addis Ababa, Ethiopia
[2] Environmental Studies Department, University of Zululand, KwaDlangezwa, South Africa

North African climate variability. Part 2: Tropical circulation systems

A. Yeshanew[1] and **M. R. Jury**[2]

With 9 Figures

Received October 12, 2005; revised March 7, 2006; accepted April 12, 2006
Published online August 31, 2006

Summary

Tropical North African climate variability is investigated using a Sahel rainfall index and streamflow of the Nile River in the 20th century. The mechanisms that govern tropical North Africa climate are diagnosed from NCEP reanalysis data in the period 1958–1998: spatially – using composite and correlation analysis, and temporally – using wavelet co-spectral analysis. The Sahelian climate is characterised by a decadal rhythm, whilst the mountainous eastern and equatorial regions exhibit interannual cycles. ENSO-modulated zonal circulations over the Atlantic/Pacific sector are important for decadal variations, and create a climatic polarity between South America and tropical North Africa as revealed through upper-level velocity potential and convection patterns. A more localised N–S shift in convection between the Sahel and Guinea coast is associated with the African Easterly Jet.

1. Introduction

One of the monsoon regions of the world is tropical North Africa (20° W–40° E and 5–15° N), where the Sahara Desert lies in contrast with the Congo basin and Gulf of Guinea. The meridional overturning circulation produces a large annual cycle. Superimposed on this basic state, large-scale variability dictates the life of the people and their socio-economic activities.

A number of researchers have investigated the Sahel climate and its slow oscillations (Lamb, 1978, 1982; Nicholson, 1981, 1998; Nicholson and Palao, 1993; Landsea et al., 1992; Nicholson and Grist, 2001). The 1950s and early 1960s are considered a wet period, followed by drought in the 1970s and 1980s. Since 1999 the drought trend has reversed. A part of the decadal variability is attributed to north–south gradients in Atlantic sea surface temperature (SST) anomalies (Folland et al., 1986; Lough, 1986; Palmer, 1986; Semazzi et al., 1996). Fontaine et al. (1995, 1998) linked to drought over the Sahel to warm El Niño-Southern Oscillation (ENSO) phase and a cool-north/warm-south Atlantic SST pattern. The atmosphere responds via subsidence from a southward extension of easterlies, a weakening of the Hadley Circulation, and a reduction of inflow from the Gulf of Guinea (Hastenrath, 2000; Camberlin et al., 2001).

Rowell et al. (1992) modelled the influence of global SST on the seasonal rainfall and simulations indicate that ocean thermodynamic effects tend to dominate the forcing. Alterations of tropical Pacific SST act to suppress (enhance) Sahel rainfall during warm (cool) ENSO phase (Palmer et al., 1992; Ward, 1992; Janicot et al., 1998); a similar association is found in southern Africa (Jury, 2003). However, the southern rains occur during the mature phase of ENSO whilst northern rains precede or follow ENSO, constraining Sahel rainfall predictions to short lead times. One of the aims of this paper is to contribute to a lengthening of lead time, through consideration of atmospheric signals that offer a stable forewarning.

At times, rainfall over the Guinea coast opposes that of the Sahel to the north (Lamb and Peppler, 1992; Rowell et al., 1995; Ward, 1998; Nicholson and Grist, 2001). Eltahir and Gong (1996) proposed an entropy mechanism for describing this variability. This theory suggests that a large meridional gradient of Atlantic SST and regional boundary-layer entropy results in a strong northward monsoon and a northward shift of the ITCZ. While a weaker Atlantic SST gradient leads to a flat distribution of entropy and a weaker monsoon (dry condition).

Ocean-atmosphere coupling may not provide a complete answer for the causes of African climate variability. The idea of positive feedback between vegetation cover, albedo, evapotranspiration and boundary layer climate has gained favour since it was first proposed in the 1970s (Charney, 1975). A number of researchers have pursued this line to better understand decadal oscillations in Sahel rainfall (Xue et al., 1990; Zeng and Eltahir, 1998; Zeng et al., 1999).

Whilst a majority of studies have concentrated on Sahel climate west of 15° E, here we focus equally on the area to the east that is characterised by higher elevations and a major river: the Nile. In recent times, the fluctuation of Nile flow has been linked to ocean-atmosphere coupling (Quinn, 1992; Eltahir and Wang, 1999; Wang and Eltahir, 1999). According to Eltahir (1996) ENSO indices account for 30% of variance of the Nile flow based on 127 years of data. From this result, Wang and Eltahir (1999) established a three month lead-time prediction model with forecast fit of 45%. Jury (2003) provided a new avenue to understand the Africa climate variability with respect to ocean-climate coupling. It was shown that African rivers fluctuate coherently across the continent and are sensitive to coupling between the zonal circulation over the tropical Atlantic, the global ENSO and Atlantic SST. According to this result, a warming in the equatorial east Pacific causes sinking motions over northern and southern Africa and a reduction of flow for all major African rivers. Here we extend that line of research.

Camberlin (1995) and Camberlin et al. (2001) considered northeast Africa climate variability and found that the occurrence of drought over Ethiopia is attributed to El Niño and high-pressure over the Arabian Sea and India. Camberlin (1997) established the association between the Southwest monsoon and northeast Africa rainfall variability and suggested that monsoon activity over India is a major trigger for boreal summer rainfall variability over the African highlands due to the outflowing TEJ and its influence on easterly wave trains. A study by Shanko and Camberlin (1998) associated the high frequency of occurrence of tropical cyclones in the Southwest Indian Ocean with Ethiopian drought, particularly during the onset season. In the study of teleconnections between tropical north Africa climate and Pacific SST (Camberlin et al., 2001), the ENSO impact on boreal summer rainfall over Ethiopia is corroborated.

The objective of this paper is to understand the circulations that modulate tropical North African climate variability. To this end, field data are analysed as discussed in Sect. 2. In Sect. 3, the spatial and temporal behaviour of tropical north African climate are outlined. The mechanisms inducing its variability are elucidated through the evaluation of composites, correlations and wavelet co-spectra. The conclusions are given in Sect. 4 within a conceptual framework.

2. Data and methods

The data and methods used to reveal North Africa climate variability are discussed here.

2.1 Data

We make use of monthly data on stream flow, rainfall, sea surface temperature (SST) and atmospheric circulation. Nile stream flow is observed at the Aswan station, Sahel rainfall is interpolated from observed, SST is observed by ships and in recent years by satellite, whilst OLR is satellite derived. The atmospheric data (wind, velocity potential, etc.) are re-analysed from observations. The nature of each variable and the sources of the data are discussed below.

Continuous monthly rainfall departures, interpolated to 0.5° resolution, were obtained from the Climate Research Unit (CRU) of the University of East Anglia. The gridded fields of rainfall were subjected to repeated rotated principal component analysis until an optimal number of clusters was identified (Jury et al., 2006). From this regionalisation, a rainfall time series for the eastern Sahel is formed and used as an index of tropical North Africa climate. Its area extends from 8–15° N, 12–32° E, centred on the lowlands of Sudan. The interannual time series is significantly correlated with rainfall from the western Sahel, hence our interpretations may be extended westward.

Continuous monthly Nile River flow data at Aswan were obtained from G. Wang (personal communication). These stream flow data are quality controlled and naturalised from known human interference (e.g. dams). These data have been used in a number of research studies (Eltahir and Wang, 1999; Eltahir, 1996; Jury, 2003). Together with rainfall, this index describes the temporal variability of tropical North African climate.

To understand the influence of ocean signals on tropical North Africa climate variability, SST data over the Pacific, Atlantic and Indian Oceans are used. These are drawn from the Reynolds reconstructed dataset. Part 1 of this paper outlines how thermocline oscillations in these basins relate to the overlying Walker circulations (Yeshanew and Jury, 2006a).

The NCEP re-analysis system assimilates all archived data from 1948 to the present via a numerical model. The details of NCEP reanalysis can be found in Kalnay et al. (1996) and Kistler et al. (2000). One the most attractive characteristics of the NCEP re-analysis with respect to climate studies is its consistency. The accuracy of re-analysis products depends on the influence of the observational data on the gridded variable. We employ wind vector and upper level velocity potential (divergence) data in our analyses.

2.2 Methods

A contingency analysis is employed with respect to East Sahel rainfall and Nile River flow for identification of wet and dry seasons (June to September). These are ranked such that the five highest and lowest years are selected for composite analysis: 1958, 1961, 1964, 1975, 1988 and 1982, 1984, 1987, 1990, 1991, respectively. A similar procedure is followed to identify extreme years for key indices of the tropical circulation.

Composite analysis was done via the NCEP/NOAA CDC web site http://www.cdc.noaa.gov/composites to obtain maps and sections at various lags and levels. Here we subtract the dry years from the wet years and plot differences for the June to September season. These fields are subsequently referred to as the wet minus dry composite. Significance tests were applied to determine if the results achieved sufficient coherence (Yeshanew, 2003), and only those that reach the 95% confidence interval are reported here.

The degree of association between two time series is estimated from the cross-correlation value, after a continuous wavelet filter (CWT) is applied to isolate climate signals in specific frequency bands, (e.g. Lau and Weng, 1995; Wang and Wang, 1996). Here we use a 1.5–16 year band filter to focus on interannual to decadal variability. CWT is used to understand the spectral energy shared by two time series and to compute how their phase lag evolves with time. Further details of the methodology can be found in Yeshanew (2003) where, in addition, the data density and quality is discussed. Our evaluation of statistical significance considers the 'deflated' degrees of freedom to account for persistence in both target and predictor records.

3. Results

Here we document results that help form an understanding of hydroclimate variability over tropical North Africa. The raw time series and spectral character for the Nile flow and East Sahel rainfall is shown in Fig. 1. The annual cycle dominates the raw data series, as expected. Peaks vary from 0.5 to 3.0 sigma from year to year. The spectral character for interannual filtered data obtains peak energy around 3 and 8 years. East Sahel rainfall exhibits a stronger decadal cycle, whilst spectral energy for the Nile flow is contained between 2 and 5 years.

3.1 Composite structure

The composite atmospheric circulation and SST structure is investigated for wet (1958, 1961, 1964, 1975, 1988) minus dry (1982, 1984, 1987,

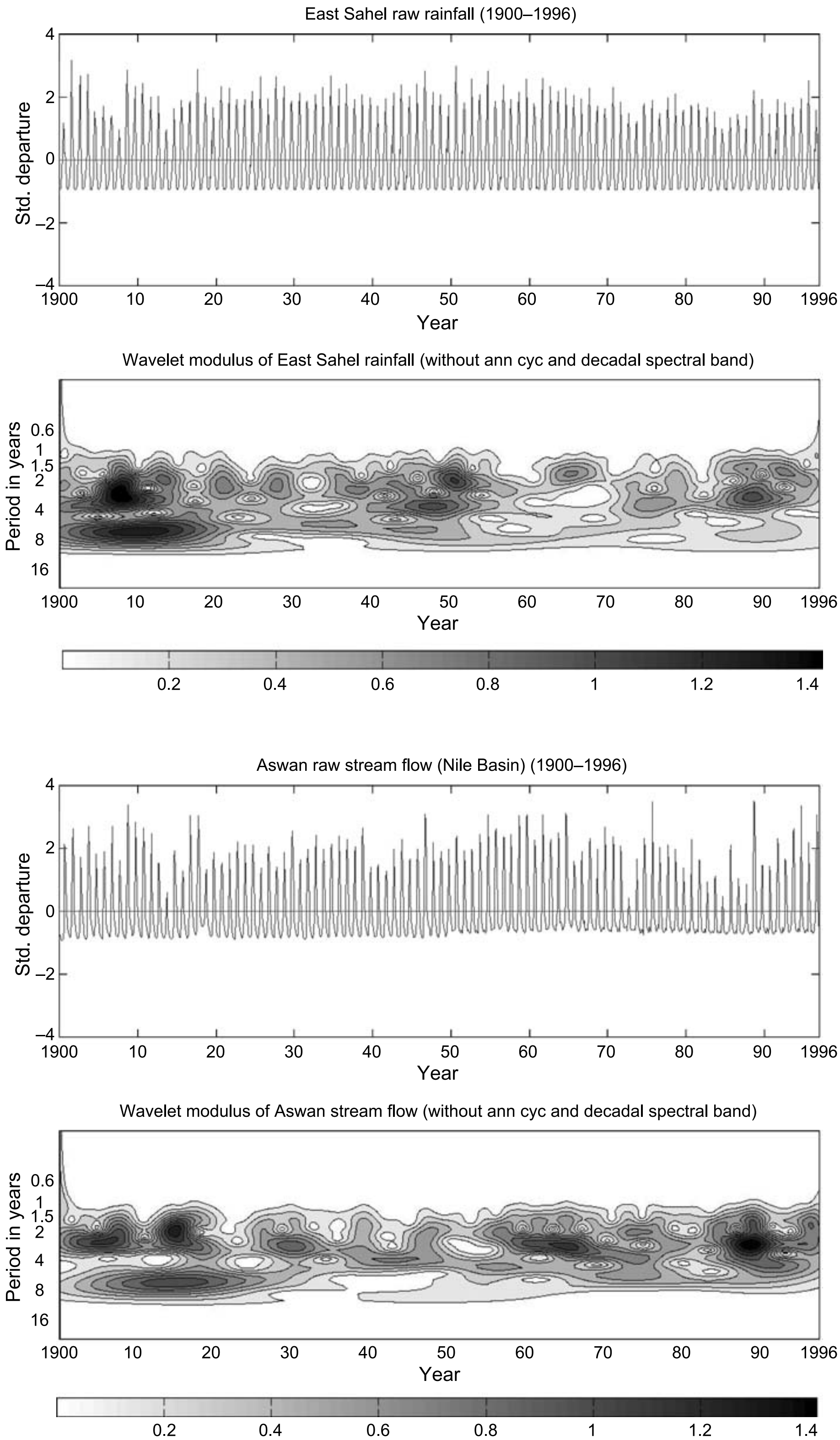

Fig. 1. East Sahel rainfall (upper) and Nile stream flow raw timeseries and interannual filtered wavelet modulus

1990, 1991) seasons. The results guide our further analysis.

The composite SST pattern exhibits a cool tongue anomaly of $<2.0\,^{\circ}C$ in the east Pacific consistent with La Nina conditions (Fig. 2a). Negative SST differences of $\sim 0.5\,^{\circ}C$ are revealed in the equatorial Indian Ocean. In the Atlantic Ocean, and the expected N–S contrast is found

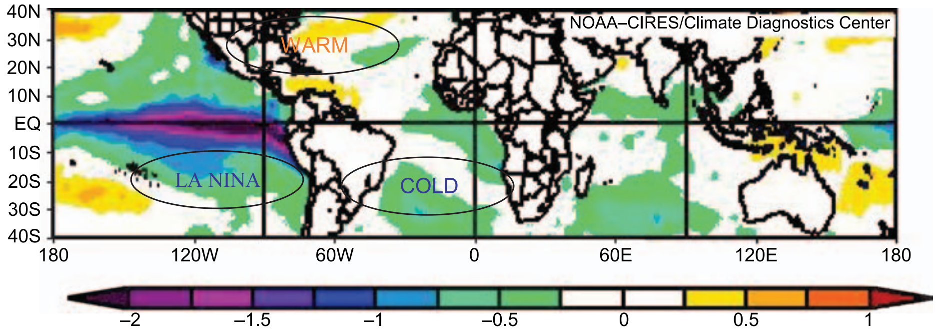

Fig. 2a. Global tropical SST pattern (°C) for wet minus dry JJAS seasons showing mainly cooler SST (Pacific La Nina) except in the north Atlantic

with SST anomaly values also $\sim \pm 0.5\,°C$. These oceanic structures are synonymous with enhanced convection over North Africa and high flow of the Nile. When composite zonal winds are considered in a vertical slice across the tropics, the pattern to emerge is two Walker Cells over the Pacific and Atlantic that overturn in opposite directions (Fig. 2b). Values are $>+3$ m/s over the Atlantic from 900 to 500 hPa and indicative of enhanced inflow from the Gulf of Guinea.

Mapping the wet minus dry composite for the 700 hPa (3 km) atmospheric circulation across the Atlantic, a low-level westerly wind is found

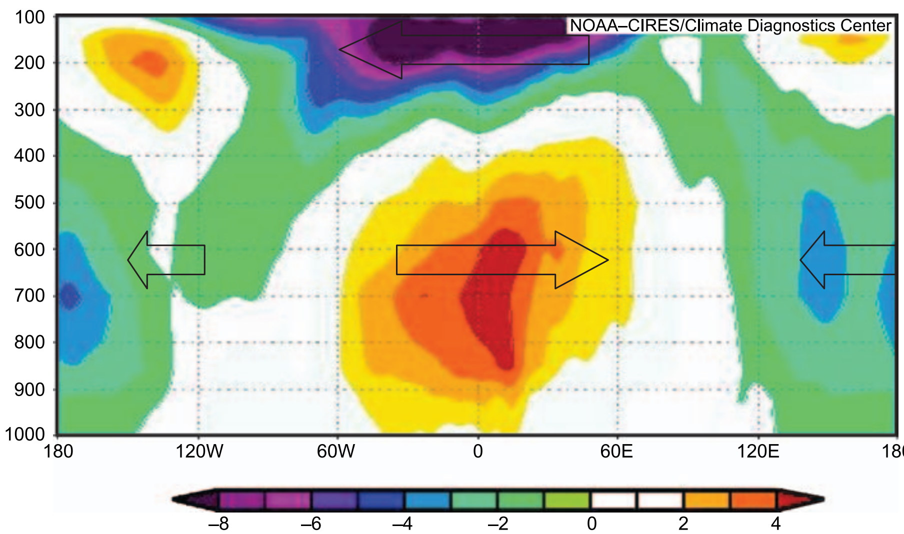

Fig. 2b. Zonal Circulation pattern for the wet minus dry composite season (m/s), averaged over the tropics 0–10° N, illustrating the Atlantic Zonal Circulation

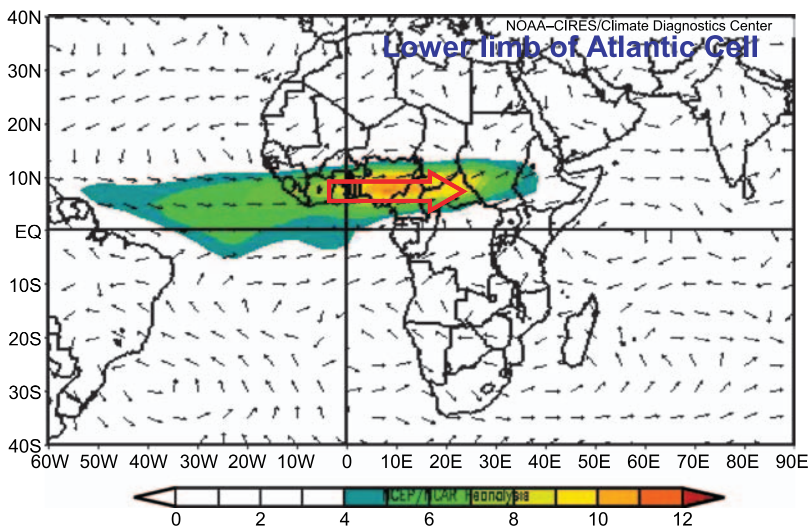

Fig. 3a. Composite winds illustrating westerly flow differences at 700 hPa (m/s). Values >4 m/s that achieve statistical significance are shaded

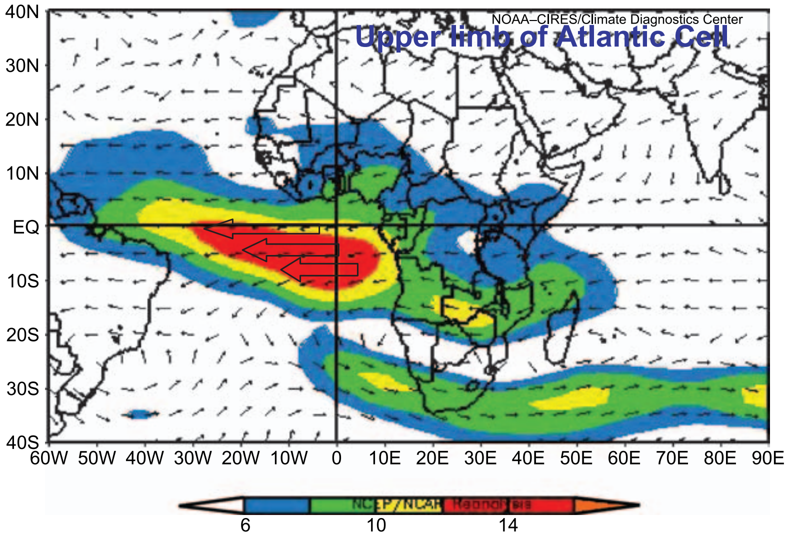

Fig. 3b. Composite winds illustrating easterly flow differences at 200 hPa (m/s). Values >6 m/s that achieve statistical significance are shaded

to extend from Brazil to Ethiopia (Fig. 3a) with a maximum over Nigeria in the 5–10° N zone. Upper easterly differences are notable (Fig. 3b) over the tropical South Atlantic. Together these suggest a zonal overturning circulation that drives African rainfall.

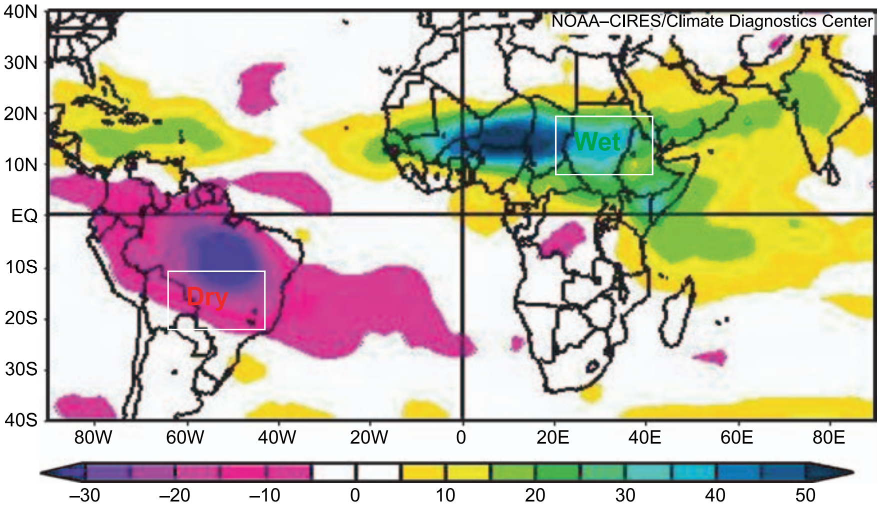

Fig. 4a. Composite OLR pattern illustrating convection polarity between tropical North Africa (enhanced convection) South America (suppressed convection) in W m^{-2}. Values $>\pm 5$ W m^{-2} that achieve statistical significance are shaded

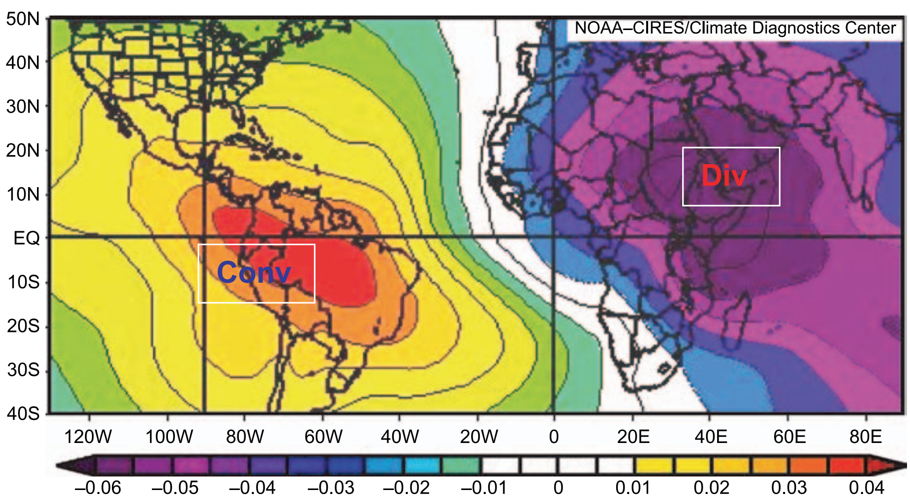

Fig. 4b. Composite upper velocity potential pattern defining the Africa–America dipole (10^6 m^2/s). Values $>\pm 10^4$ m^2/s that achieve statistical significance are shaded

Tropical rainfall is well detected by outgoing long-wave radiation. Our composite wet minus dry field (Fig. 4a) illustrates enhanced convection over tropical North Africa and, surprisingly, suppressed convection over South America. This represents a remarkable convective polarity between the two continents. Similarly the upper level velocity potential composite in Fig. 4b displays two distinct centres of action on either side of the tropical Atlantic, in agreement with Jury (2003). Statistical significance tests for various SST and atmospheric indices (Yeshanew, 2003) support the idea of coupling between the Atlantic zonal overturning circulation, Pacific ENSO and Atlantic N–S SST gradient. Cross-correlation of the interannual-filtered velocity potential time series for tropical North Africa and South America achieves a significant negative correlation (−0.87). It seems that local terrestrial conditions play a secondary role, as the two opposing centres of action form an integral part of the Atlantic ENSO response. We will refer to this as the Africa–America dipole.

There are local differences in the uptake of this signal. To reveal this, strong minus weak years of the African Easterly Jet (AEJ) are considered, based on the 600-hPa zonal winds averaged over 5–15° N, 10° W–20° E. The mid-level vertical velocity field (Fig. 5) reveals a strong N–S contrast as expected (Nicholson and Grist, 2001). There are ascending and descending cells in the equatorial region and over Africa around 15° N, respectively. Hence when the AEJ is strong, it may suppress uptake of the larger east–west dipole. Further analysis of this aspect is beyond the scope of our paper.

3.2 Temporal analyses

In this section the interaction of key atmospheric circulations is studied, with particular attention given to coupling of the Atlantic Zonal Circulation and Pacific Walker Cell. Their opposing circulations generate an 'atmospheric bridge' (Tseng, 1999) that transmits the ENSO signal globally. Of the indices tested, tropical North

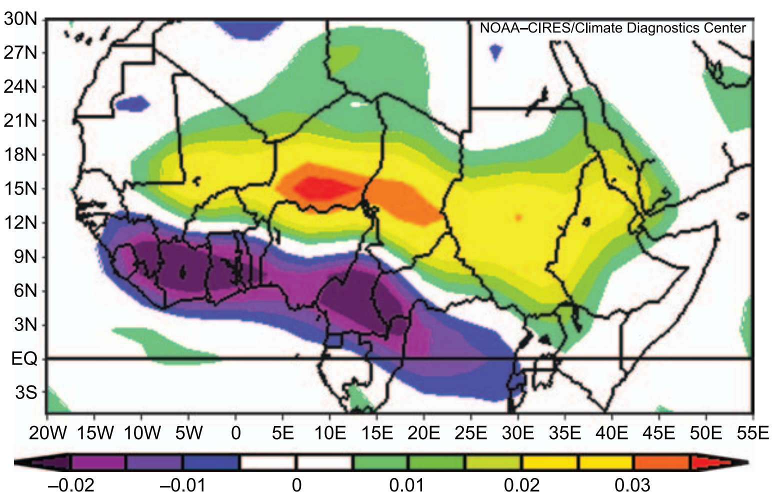

Fig. 5. 500 hPa vertical velocity (Pa s^{-1}) for strong minus weak AEJ composite illustrating opposing conditions for Guinea and Sahel regions. Values $> \pm 0.005$ Pa s^{-1} that achieve statistical significance are shaded

Table 1. Key atmospheric circulation indices used in the study

Variable	Name	Area
Equatorial Atlantic 700-hPa zonal wind	eqaU700	40° W–15° E; 10° S–10° N
Equatorial Atlantic 200-hPa zonal wind	eqa200	40° W–15° E; 10° S–10° N
Atlantic Zonal Circulation	aCIR = eqaU700 − eqU200	40° W–15° E; 10° S–10° N
Transverse Indian Monsoon Circulation	mCIR = niU850 − TEJ150	niU850: 50–75° E; 5–20° N TEJ150: 50–90° E; 5–20° N
Tropical Pacific 1000-hPa zonal wind	tpU1000	180–75° W; 20° S–20° N
Tropical Pacific 300-hPa zonal wind	tpU300	180–75° W; 20° S–20° N
Walker Circulation	wCIR = tpU300 − tp1000	180–75° W; 20° S–20° N

Africa climate is associated with the Atlantic Zonal Circulation and the Transverse Indian Monsoon (Webster et al., 1998). Indices representing these circulations are listed in Table 1.

Linear regression models are developed based on continuous monthly data from 1950 to 1998 ($N = 588$). Useful results are obtained from this analysis and the models and explained variance are given in Table 2. In the algorithms, the anti-phase Atlantic and Pacific circulation indices act as zero lag 'signals' with respect to rainfall. The Indian Transverse Monsoon index accounts for a significant portion of climate variability, parti-

Table 2. Association between Zonal Circulations and N. Africa/Brazil climate

a) Atlantic and Pacific Walker Circulations
East-Sahel-rainfall = 0.61(aCIR) − 0.44(wCIR), $r^2 = 75\%$
Guinea-coast-rainfall = 0.35(aCIR) − 0.56(wCIR), $r^2 = 48\%$
Nile-River-flow = 0.55(aCIR) − 0.41(wCIR), $r^2 = 50\%$
Brazil-rainfall = − 0.32(aCIR) + 0.53(wCIR), $r^2 = 41\%$
b) Transverse Indian Monsoon Circulation
East-Sahel-rainfall = 0.91(mCIR), $r^2 = 83\%$
Guinea-coast-rainfall = 0.80(mCIR), $r^2 = 48\%$
Nile-River-flow = 0.57(mCIR), $r^2 = 32\%$
Brazil-rainfall = − 0.91(mCIR), $r^2 = 83\%$

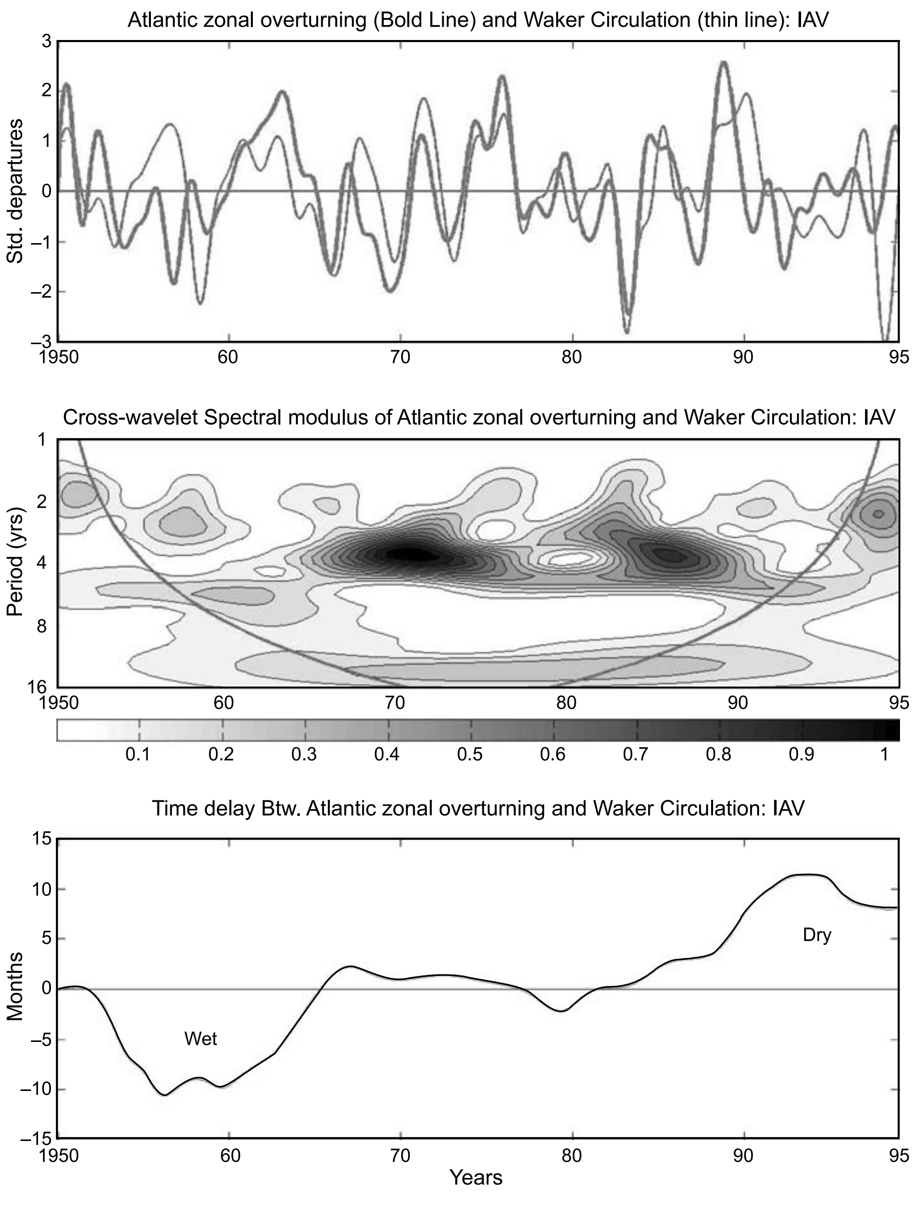

Fig. 6. Co-spectral analysis and phase relationship between the Atlantic Zonal Circulation and Pacific Walker Circulation. Wet and dry periods of tropical North Africa rainfall are labeled. Negative time delay refers to Pacific leading Atlantic

cularly in respect of the east Sahel rainfall. Due to co-linearity it remains independent from the other indices in our analyses.

To understand time evolution of spectral energy shared by the tropical circulation and climatic indices, cross-spectra and phase analyses are applied to interannual filtered data.

The Atlantic and Pacific zonal circulations co-vary with time and achieve a statistical significant correlation at lags ±6 months. Common spectral power resides near four years. Decadal co-spectra achieve one-third the strength. The amplitude of the four year cycle is strong from 1965 to 1990 (Fig. 6), but the phase relationship varies. The Pacific circulation leads the Atlantic (up to 10 months) from 1950 to 1965. The coupling is weak from 1965 to 1980, whereafter the Atlantic leads. This may be an important finding as regards the coupling of African climate with the surrounding oceans. Wet epochs of Sahel rainfall occur when the Pacific is overturning lower easterly/upper westerly and leading the Atlantic. The dry period in the Sahel corresponds with the Atlantic leading and overturning lower easterly/upper westerly. Further consideration is given to this aspect in Sect. 4.

The filtered time series and co-spectral characteristics for the Atlantic zonal circulation and east Atlantic SST are compared in Fig. 7. Whilst there is some shared spectral power at

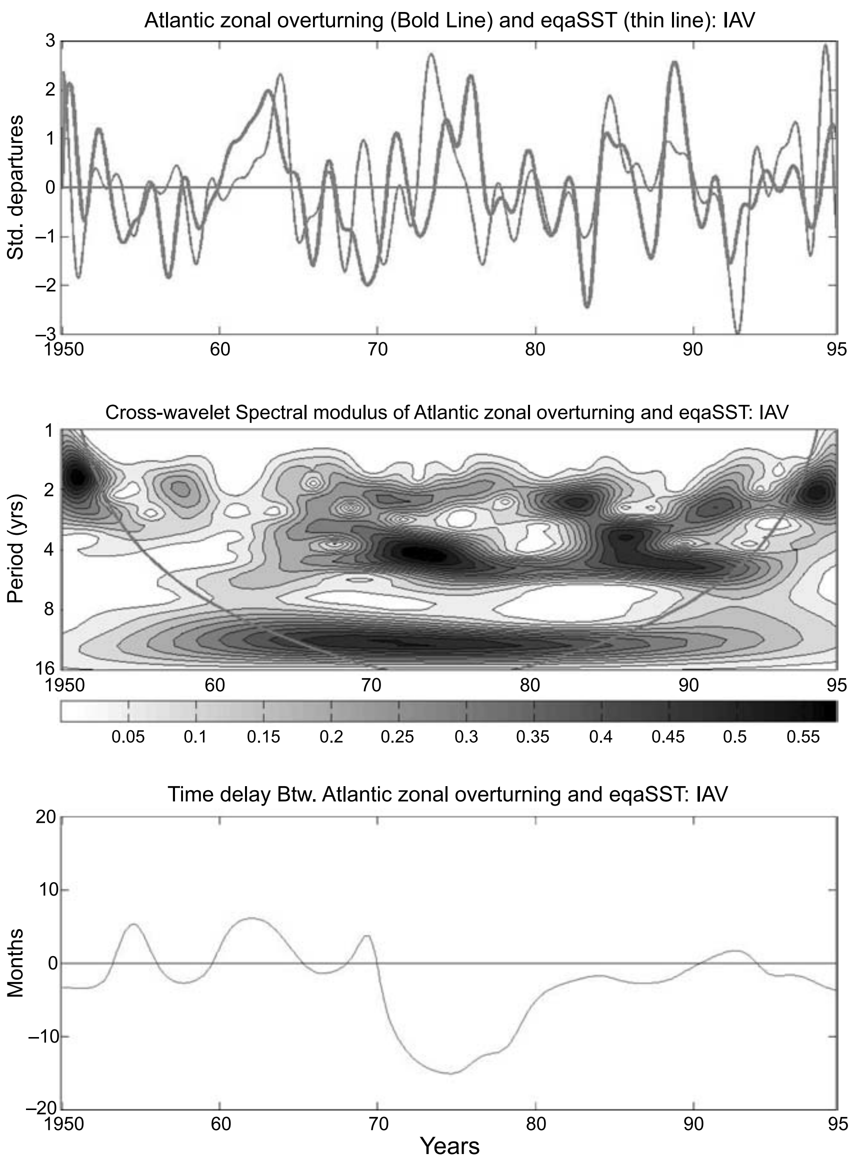

Fig. 7. Co-spectral analysis and phase relationship between Atlantic Zonal Circulation and equatorial Atlantic 2SST. Negative time delay refers to ocean leading atmosphere

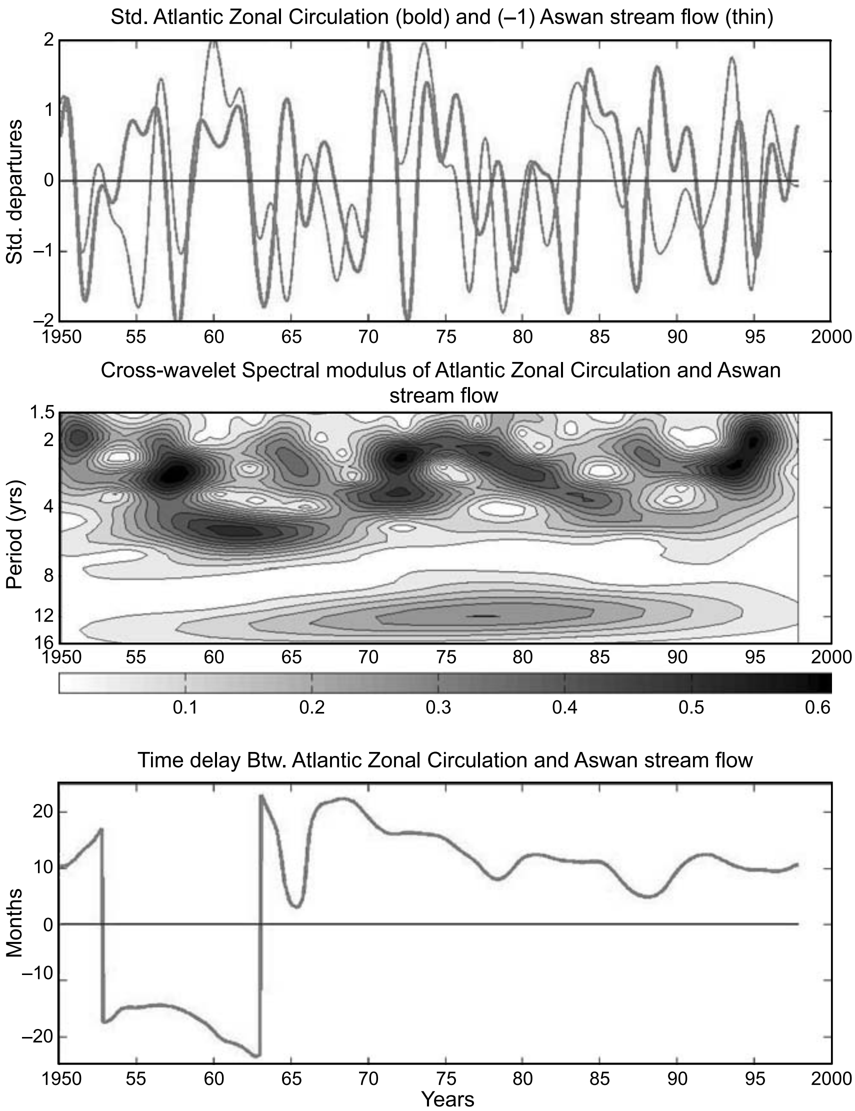

Fig. 8. Co-spectral wavelet transform between Atlantic Zonal Circulation and Nile stream flow. The Atlantic Circulation leads the Nile flow except from 1953 to 1963 (e.g. negative time delay)

4 years, there is significantly more spectral energy in the decadal time scale than found in the Pacific–Atlantic link illustrated above. Indeed the $\sim$4 and $\sim$10 year spectral power is nearly equal. The phase lag is stable and nearly simultaneous except during the 1970s when SST leads.

The Atlantic zonal circulation is compared with the Nile River flow (Fig. 8). The wavelet analysis reveals a shared spectral energy around 3 years, alternating between 2 and 4 years. The phase relationship suggests that the Atlantic circulation leads the Nile flow except in the first decade, when 5–6 year cycles are present. The lead time is $\sim$10 months throughout the record, considerably longer than that afforded by SST alone (Ward, 1998).

4. Discussion and conclusion

Understanding the physical mechanisms of climate variability across tropical North Africa is the aim of this study. Wavelet spectral analysis has revealed that the Nile River flow possesses a high frequency signal, whereas decadal fluctuations dominate Sahel rainfall to the west. The rhythm appears dependent on elevation: the Nile flow originating from the 2000 m Ethiopian plateau, the east Sahel rains falling on land that is <500 m. Here we have focused on zonal interactions, whilst recognising the importance of meridional links, e.g. west Sahel rainfall and the Atlantic multi-decadal oscillation (Enfield et al., 2001) (www.cdc.noaa.gov/Correlation).

We find that coupling of the Atlantic zonal circulation and Pacific Walker Cell is an impor-

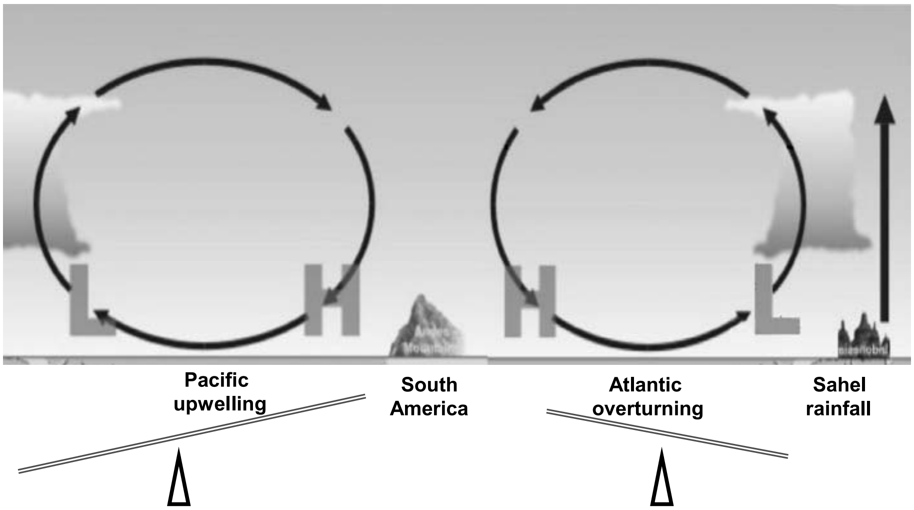

Fig. 9. Schematic diagram showing the zonal overturning circulations over the Pacific and Atlantic during a wet year over North Africa/dry year over South America. The associated thermocline 'see-saw' is illustrated

tant influence on tropical North African climate (illustrated in Fig. 9). These east–west circulations result in two opposing centres of action on either side of the tropical Atlantic, giving rise to convective polarity between tropical North Africa and South America. The Africa–America dipole helps define Walker cell adjustment with respect to ENSO (Giannini et al., 2003). Whilst conceptual models often depict two cells over the Pacific during warm phase and one cell in cold phase, here we found single cells over the Atlantic and Pacific that reverse from warm to cold phase.

The Atlantic Zonal Circulation and Sahelian rainfall exhibit shared spectral energy at 3–8 year cycles, particularly during the period when the Atlantic circulation leads the Pacific. Our study found three epochs: Pacific Walker Cell leading (1950–1970, wet phase in Sahel), passive coupling (1970–1980, dry period in Sahel), and Atlantic leading (after 1980). During the passive phase, the Atlantic Zonal Circulation interacts with the underlying equatorial Atlantic SST. The Atlantic-Pacific ENSO coupling also impacts on the Indian Transverse Monsoon (Yeshanew, 2003). The Transverse Monsoon is associated with Indo-Pacific SST and its ocean Rossby wave activity (White, 2001). With a phase speed of $0.07\,m\,s^{-1}$, the low frequency 'see saw' of the Pacific thermocline has a rhythm that is consistent with the observed alternation of the Africa–America dipole and climate variability on both sides of the tropical Atlantic (Yeshanew and Jury, 2006a).

Although east–west overturning circulations modulate the convection polarity between tropical North Africa and South America, the AEJ determines a more local-scale meridional overturning. A strong AEJ causes a shift in convection from the Sahel to the Guinea Coast.

A pivotal issue that is addressed here is the potential for a global tropical teleconnection. Our analysis indicates the Atlantic and Pacific Walker Cells operating like 'gears' with a rhythm modulated by ENSO. From our work it is suggested that kinematic variables may prove quite useful in statistical forecasts of Sahelian climate, providing longer lead times than thermodynamic parameters. Predictability is the focus of part 3 of this paper (Yeshanew and Jury, 2006b).

Acknowledgment

The data used in this study were obtained from National Centre for Environmental Prediction, and G. Wang, Mass. Inst. Technology.

References

Camberlin P, Jaincot S, Poccard I (2001) Seasonal and atmospheric dynamics of the teleconnection between African rainfall and tropical seas-surface temperature: Atlantic vs. ENSO. Int J Climatol 21: 973–1005

Camberlin P (1995) June–September rainfall in Northeast Africa and atmospheric signals over the tropics: A zonal perspective. Int J Climatol 15: 773–783

Camberlin P (1997) Rainfall anomalies in the source region of the Nile and their connection with Indian summer monsoon. J Climate 10: 1380–1392

Charney JG (1975) Dynamics of desert and drought in the Sahel. Quart J Roy Meteor Soc 101: 193–202

Eltahir EAB, Wang G (1999) Nilometers, El Niño and climate variability. Geophys Res Lett 26(4): 489–492

Eltahir EAB (1996) El Niño and the natural variability in the flow of the Nile. Water Resour Res 32: 131–137

Eltahir EAB, Gong C (1996) Dynamics of wet and dry years in West Africa. J Climate 9: 1030–1042

Enfield DB, Mestas-Nunez AM, Trimble PJ (2001) The Atlantic multidecadal oscillation and it's relation to rainfall and river flows in the continental U.S. Geophys Res Lett 28: 2077–2080

Folland CK, Palmer TN, Parker DE (1986) Sahel rainfall and world-wide sea temperature, 1901–85. Nature 320: 602–607

Fontaine B, Janicot S, Moron V (1995) Rainfall anomaly patterns and wind field signals over West Africa in August(1958–1989). J Climate 8: 1503–1510

Fontaine B, Trzaska I, Janicot S (1998) Evolution of the relationship between near global and Atlantic SST mode and the rainy season in West Africa: Statistical analyses and sensitivity experiments. Climate Dynamics 14: 353–368

Giannini A, Saravanan R, Chang P (2003) Oceanic forcing of Sahel rainfall on interannual to interdecadal time scales. Science 302: 1027–1030

Hastenrath S (2000) Interannual and longer-term variability of upper air circulation over the tropical Atlantic and West Africa in boreal summer. Int J Climatol 20: 1415–1430

Janicot S, Harxallah A, Fontaine B, Moron V (1998) West African monsoon dynamic and eastern equatorial Atlantic and Pacific SST anomalies (1970–1988). J Climate 11: 1874–1882

Jury MR (2003) Coherent variability of African River flows, composite climate structure and the Atlantic circulation. Water SA 29(1): 1–10

Jury MR, Rautenbach H, Tadross M, Philipp A (2006) Evaluating spatial scales of climate variability in sub-Saharan Africa. Theor Appl Climatol (in press)

Kalnay E, Kanamitsu M, Kistler R, Collins W, Deaven D, Gandin L, Iredell M, Saha S, White G, Woollen J, Zhu Y, Leetmaa A, Reynolds R, Chelliah M, Ebisuzaki W, Higgins W, Janowiak J, Mo KC, Ropelewski C, Wang J, Jenne R, Joseph D (1996) The NCEP/NACR reanalysis 40-year project. Bull Amer Meteor Soc 77: 437–471

Kistler EK, Collins W, Saha S, White G, Woolen J, Chelliah M, Ebisuzaki W, Kanamitsu M, Kousky V, van den Dool H, Jenne R, Fiorino M (2000) The NCEP/NCAR 50 year reanalysis. Bull Amer Meteor Soc 82(2): 247–268

Lamb PJ (1978) Large-scale tropical Atlantic circulation patterns associated with Subsaharan weather anomalies. Tellus 30: 240–251

Lamb PJ (1982) Persistence of Subsaharan drought. Nature 299: 46–48

Lamb PJ, Peppler RA (1992) Further case studies of tropical Atlantic surface atmospheric and oceanic patterns associated with sub-saharan drought. J Climate 5: 476–488

Lau K-M, Weng H-Y (1995) Climate signal detection using wavelet transform: How to make a time series sing. Bull Amer Meteor Soc 76: 2391–2402

Lough JM (1986) Tropical Atlantic seas surface temperatures and rainfall variations in sub-saharan Africa. Mon Wea Rev 114: 561–570

Nicholson SE (1981) Rainfall and atmospheric circulation during drought periods and wetter years in West Africa. Mon Wea Rev 109: 2191–2208

Nicholson SE, Palao IM (1993) A re-evaluation of rainfall variability in the Sahel. Part I: characteristics of rainfall fluctuations. Int J Climatol 13: 371–289

Nicholson SE, Grist JP (2001) A conceptual model for understanding rainfall variability in the West African Sahel on interannual and interdecadal timescale. Int J Climatal 21: 1733–1757

Palmer TN (1986) Influence of Atlantic, Pacific, and Indian Oceans on Sahel rainfall. Nature 322: 251–253

Palmer TN, Brankovic C, Viterbo P, Miller MJ (1992) Modeling the interannual variation of summer monsoon. J Climate 5: 299–417

Quinn WH (1992) A study of southern oscillation-related climate activity 622–1990 incorporating Nile river flood data. In: Diaz HF, Markgraf V (eds) El Niño: Historical and paleoclimae aspects of Southern Oscillation. pp 119–142

Rowell DP, Folland CK, Maskell K, Ward JA, Ward MN (1992) Modelling the influence of global sea surface temperatures on the variability and predictability of seasonal Sahel rainfall. Geophys Res Lett 19: 905–908

Rowell DP, Folland CK, Maskell K, Ward JA, Ward MN (1995) Variability of summer rainfall over tropical North Africa (1906–92): Observation and modelling. Quart J Roy Meteor Soc 121: 669–704

Semazzi HFM, Burns B, Lin NH, Schemm JE (1996) A GCM study of teleconnections between the continental climate of Africa and global sea surface temperature. J Climate 9: 2480–2497

Shanko D, Camberlin P (1998) The effect of southwest Indian Ocean tropical cyclone on Ethiopian drought. Int J Climatol 18: 1373–1388

Wang B, Wang Y (1996) Temporal structure of the southern oscillation as revealed by waveform and wavelet analysis. J Climate 9: 1586–1598

Wang G, Eltahir EAB (1999) Use of information in the medium-and long-range forecasting of the Nile floods. J Climate 12: 1726–1737

Ward MN (1992) Worldwide ocean-atmosphere surface fields and Sahelian rainfall variability. J Climate 5: 454–475

Ward MN (1998) Diagnosis and short-lead time prediction of summer rainfall in tropical north Africa at interannual and multi-decadal timescales. J Climate 11: 3167–3191

Webster PJ, Magana VO, Palmer TN, Shukla J, Tomas RA, Yanai M, Yasunari T (1998) Monsoons: Processes, predictability, and the prospects for prediction. J Geophys Res 103(c7) (TOGA issue): 14451–14510

White WB (2001) Evidence of coupled Rossby Waves in the annual cycle of the Indo-Pacific Ocean. J Phys Oceanogr 31: 2944–2957

Xue Y, Liu KN, Kasahara A (1990) Investigation of biogeophysical feedback on African climate using a two-dimensional model. J Climate 3: 337–352

Yeshanew A (2003) Mechanisms and prediction of climate variability in tropical North Africa. PhD thesis, University of Zululand (South Africa), pp 546

Yeshanew A, Jury MR (2006a) North African climate variability, part 1: Tropical thermocline coupling. Theor Appl Climatol (in press)

Yeshanew A, Jury MR (2006b) North African climate variability, part 3: resource prediction. Theor Appl Climatol (in press)

Zeng N, Eltahir EAB (1998) The role of vegetation in the dynamics of West African monsoons. J Climate 11: 2078–2096

Zeng N, Neelin JD, Lau KM, Tucker CJ (1999) Enhancement of interdecadal climate variability in the Sahel by vegetation interaction. Science 286: 1537–1540

Authors' addresses: Abebe Yeshanew, National Meteorological Services Agency, Addis Ababa, Ethiopia; Mark R. Jury* (e-mail: jury@uprm.edu), Environmental Studies Department, University of Zululand, KwaDlangezwa 3886, South Africa; *Current address: Physics Department, University of Puerto Rico, Mayaguez, PR 00681-9016, USA.